Virology 538 (2019) 53–60

Contents lists available at ScienceDirect

Virology

journal homepage: www.elsevier.com/locate/virology

Cancer susceptibility of beta HPV49 E6 and E7 transgenic mice to 4-nitroquinoline 1-oxide treatment correlates with mutational signatures of tobacco exposure

Daniele Viarisio[a], Alexis Robitaille[b], Karin Müller-Decker[a], Christa Flechtenmacher[c], Lutz Gissmann[a,d], Massimo Tommasino[b,*]

[a] Deutsches Krebsforschungszentrum (DKFZ), Im Neuenheimer Feld 280, 69120, Heidelberg, Germany
[b] International Agency for Research on Cancer (IARC), World Health Organization, 150 Cours Albert Thomas, 69372, Lyon Cedex 08, France
[c] Department of Pathology, University Hospital of Heidelberg, Im Neuenheimer Feld 220, 69120, Heidelberg, Germany
[d] Department of Botany and Microbiology (honorary MMember), King Saud University, Riyadh, Saudi Arabia

ARTICLE INFO

Keywords:
Beta HPV types
Upper-digestive tract cancer
4-Nitroquinoline 1-oxide
Mutational signatures of tobacco exposure

ABSTRACT

We have previously showed that a transgenic (Tg) mouse model with cytokeratin 14 promoter (K14)-driven expression of E6 and E7 from beta-3 HPV49 in the basal layer of the epidermis and of the mucosal epithelia of the digestive tract (K14 HPV49 E6/E7 Tg mice) are highly susceptible to upper digestive tract carcinogenesis upon exposure to 4-nitroquinoline 1-oxide (4NQO). Using whole-exome sequencing, we show that in K14 HPV49 E6/E7 Tg mice, development of 4NQO-induced cancers tightly correlates with the accumulation of somatic mutations in cancer-related genes. The mutational signature in 4NQO-treated mice was similar to the signature observed in humans exposed to tobacco smoking and tobacco chewing. Similar results were obtained with K14 Tg animals expressing mucosal high-risk HPV16 E6 and E7 oncogenes. Thus, beta-3 HPV49 share some functional similarities with HPV16 in Tg animals.

1. Introduction

Human papillomaviruses (HPV) are a large family of double-stranded DNA viruses that infect the mucosal and cutaneous epithelia. They are classified in a phylogenetic tree in genera, based on nucleotide sequence homology of the major capsid protein L1 (Van Doorslaer et al., 2013). Genus alpha HPV types have been most studied so far, because a subgroup, the mucosal alpha high-risk (HR) HPV types, is responsible for the development of cervical cancer and a subset of other anogenital and oropharyngeal cancers. The products of two early genes, E6 and E7, are the key oncoproteins of HPV (Tommasino, 2014). In addition to alpha HPV types, genus beta HPVs also appear to be associated with human carcinogenesis. Beta HPV types are subdivided into five different species (beta-1–5), of which beta-1 and beta-2 are the largest subgroups (Van Doorslaer et al., 2011). They are abundantly present on the skin, and many findings support their role, together with ultraviolet (UV) radiation, in the development of cutaneous squamous cell carcinoma (cSCC) (Rollison et al., 2019). Accordingly, mechanistic studies have well demonstrated the transforming properties of E6 and E7 from a few beta-1 and beta-2 HPV types (e.g. HPV8 and HPV38) in *in vitro* and *in vivo* experimental models (reviewed in refs. (Tommasino, 2017; Hasche et al., 2018). In particular, these viral oncoproteins are able to promote proliferation and to circumvent cellular stresses induced by UV radiation. These findings indicate that in the context of the natural infection, beta HPV E6/E7 expression keeps cells alive despite the accumulation of UV-induced DNA mutations. As a consequence, beta HPV-infected keratinocytes may acquire a high probability of progressing towards cellular transformation. Thus, beta HPVs act as facilitators of the accumulation of UV-induced DNA mutations, but they are not the main drivers. In agreement with this model, findings indicate that beta HPV types are necessary at an early stage of carcinogenesis and are dispensable for the maintenance of the cancer phenotype (Rollison et al., 2019).

In addition to the skin, beta HPV types can be found at other anatomical sites, including the mucosal epithelia (Bottalico et al., 2011; Forslund et al., 2013; Hampras et al., 2017; Pierce Campbell et al., 2013; Torres et al., 2015). In particular, beta-3 HPV types, i.e. HPV types 49, 75, 76, and 115, appear to preferentially infect the mucosal

* Corresponding author. Infections and Cancer Biology Group, International Agency for Research on Cancer, World Health Organization, 150 Cours Albert Thomas, 69372, Lyon Cedex 08, France.
E-mail address: tommasino@iarc.fr (M. Tommasino).

https://doi.org/10.1016/j.virol.2019.09.010
Received 18 June 2019; Received in revised form 20 September 2019; Accepted 23 September 2019
Available online 24 September 2019
0042-6822/ © 2019 Published by Elsevier Inc.

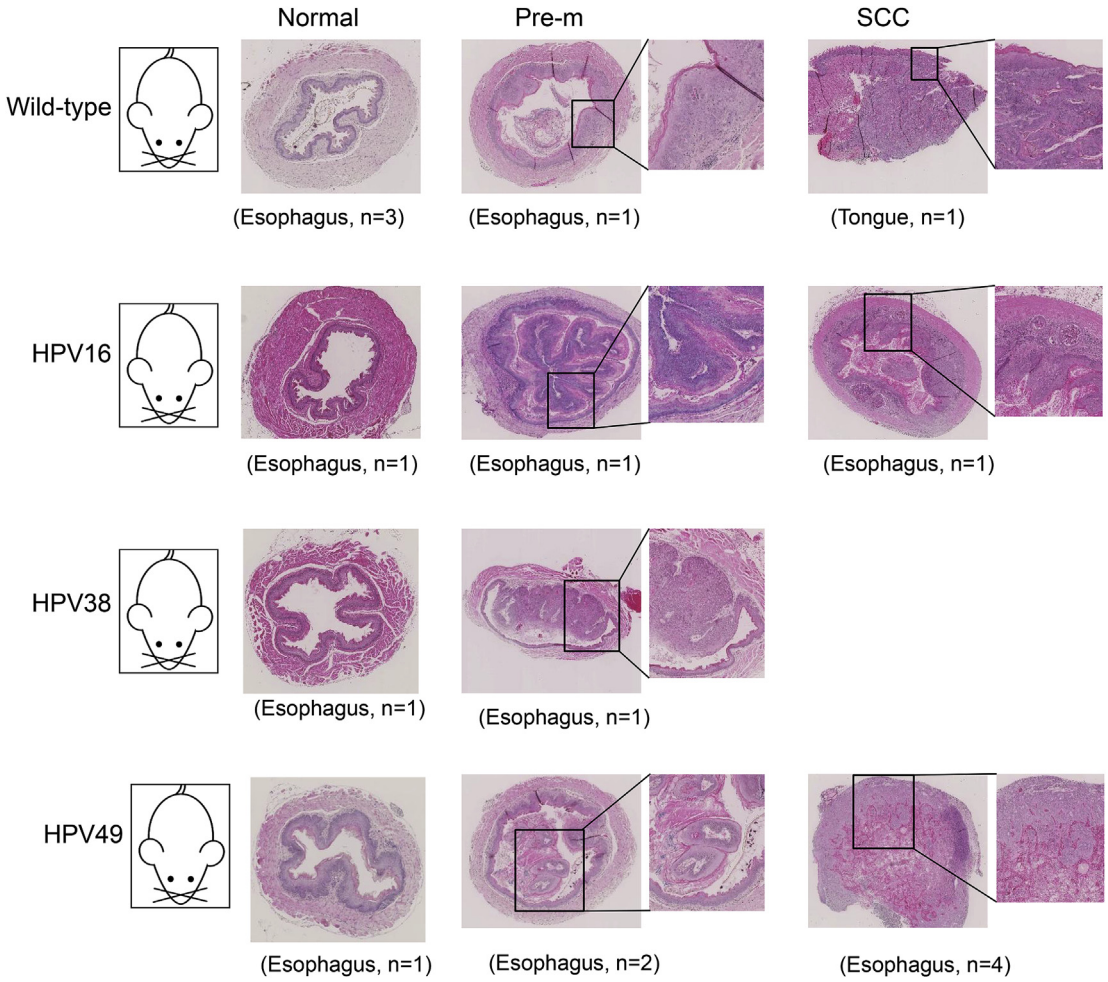

Fig. 1. Representative images of H&E-stained sections from WT or Tg mice from which the genomic DNA was extracted for whole-exome sequencing. Normal tissue, pre-malignant lesions (Pre-m), and squamous cell carcinoma (SCC) from the indicated mice exposed to long-term 4NQO treatment were collected for DNA extraction. Tissues were also processed for histological analyses. The text in brackets indicates the anatomical site, followed by the number of specimens from independent animals used for the whole-exome sequencing. From left to right, sections of unaffected esophagus, sections of esophagus affected by Pre-m lesions characterized by medium grade dysplasia (WT, HPV16, HPV49 E6/E7 Tg mice) or high grade dysplasia (HPV38 E6/E7 Tg mouse), and sections of invasive SCC from the tongue of a WT mouse and from the esophagus of HPV16 and HPV49 E6/E7 Tg mice. The stained sections were first scanned with a 5 × enlargement and then zoomed in via software analysis.

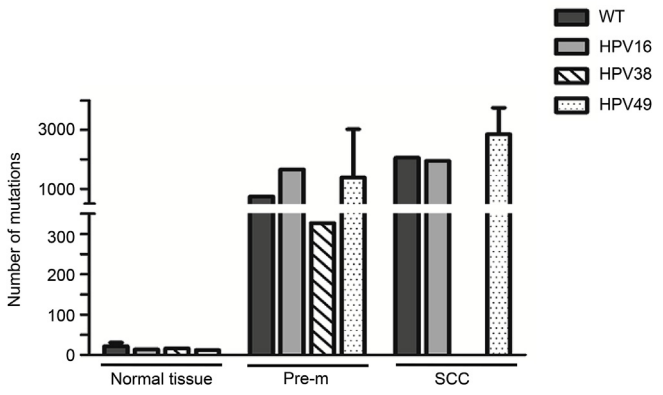

Fig. 2. The number of 4NQO-induced DNA mutations varies in the WT and different K14 HPV E6/E7 Tg animals. After whole-exome sequencing, the numbers of somatic mutations (SNPs and indels) were determined that have a functional impact and fall in exonic or splicing regions, and have an allelic fraction of 5% or more. The differences in mutation numbers between the different animal models are statistically significant: normal versus Pre-m, $P = 0.004$; Normal versus SCC, $P = 0.002$; Pre-m versus SCC, $P = 0.05$. Bars indicate standard deviations.

epithelia compared with the skin (Forslund et al., 2013; Hampras et al., 2017).

Functional studies showed that E6 and E7 from beta-3 HPV49 and the mucosal HR HPV16 share some functional similarities (Cornet et al., 2012; Viarisio et al., 2016). Similarly to what has been observed in HPV16 E6/E7 transgenic (Tg) mice (Strati et al., 2006), K14-driven expression of HPV49 E6 and E7 in mouse epithelia resulted in elevated susceptibility to upper digestive tract carcinogenesis upon initiation with the tobacco-mimicking and DNA-damaging agent 4-nitroquinoline 1-oxide (4NQO) (Viarisio et al., 2016; Ikenaga et al., 1975). However, these Tg mice did not show an increased susceptibility to chronic UV irradiation compared with the wild-type (WT) animals. Vice versa, beta-2 HPV38 E6 and E7 expression in K14 HPV38 E6/E7 Tg mice strongly cooperates with UV radiation in the development of cSCC, but the mice were little affected by 4NQO treatment (Viarisio et al., 2011, 2016). In the case of K14 beta-2 HPV38 E6/E7 Tg mice, the high cSCC incidence upon long-term UV exposure tightly correlates with their tendency to accumulate the classic UV-induced DNA mutational profile (Viarisio et al., 2018), further supporting the model described above for the role of the beta-1 and beta-2 HPVs as facilitators of UV-mediated skin carcinogenesis. A similar scenario could be hypothesized in the cooperation of beta-3 HPV49 E6 and E7 and 4NQO in promoting upper

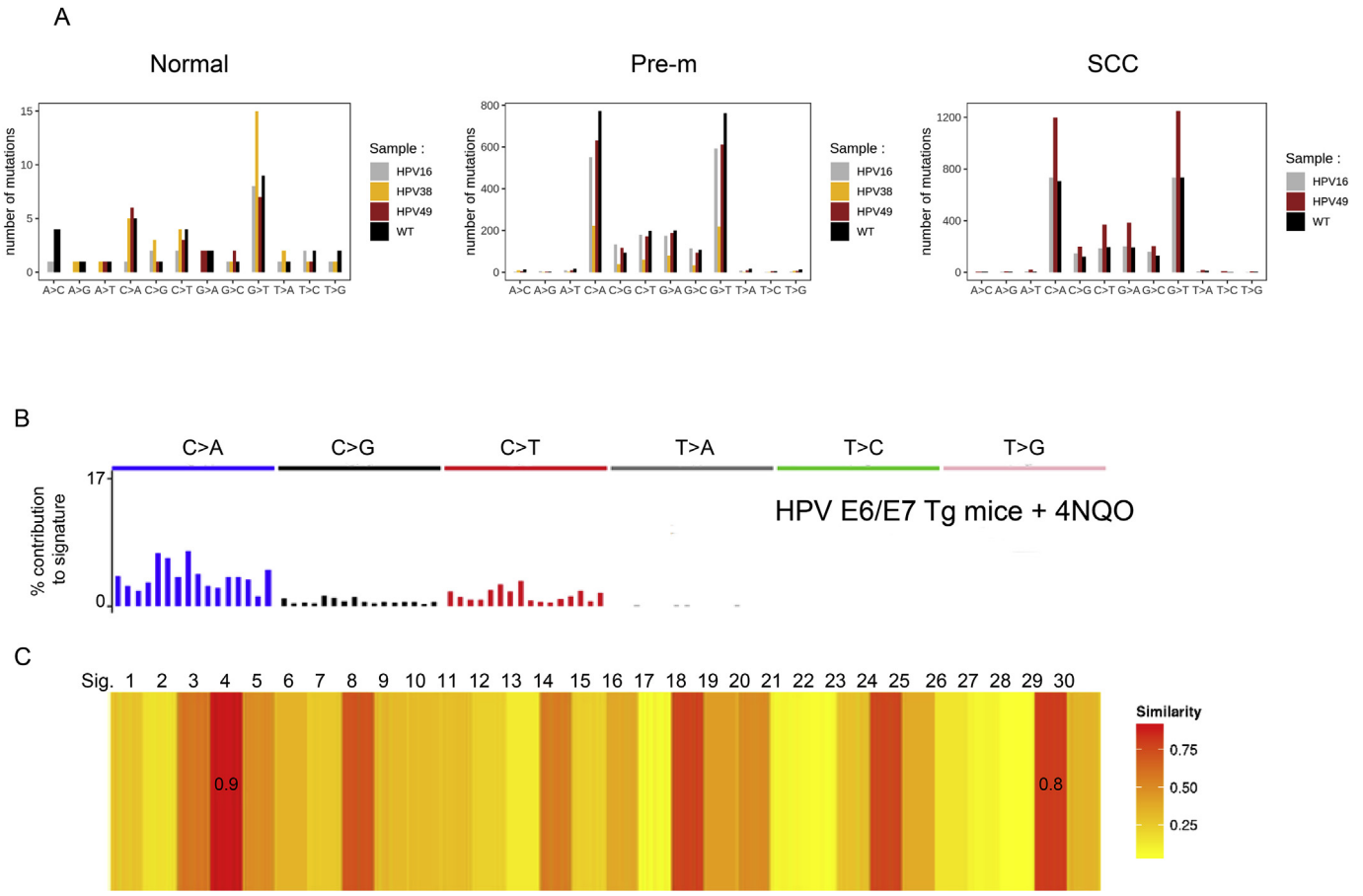

Fig. 3. 4NQO-induced DNA mutations increase with the severity of upper digestive tract lesions in the different K14 HPV E6/E7 Tg animals. (**A**) Different types of DNA mutations detected in upper digestive tract normal tissue, pre-malignant lesions (Pre-m), and squamous cell carcinoma (SCC) in Tg animals exposed to long-term 4NQO treatment. (**B**) SCCs of K14 HPV49 E6/E7 Tg mice treated with 4NQO display a clear tobacco-induced mutational signature with a very high number of C:G > A:T mutations. This type of mutation makes up the majority of the single-nucleotide variant types in Pre-m and SCC samples from the WT and Tg animals. The *y* axis shows the percentage contribution of those mutations to signatures, and the *x* axis shows the trinucleotide sequence context. (**C**) Heatmap presenting the similarity of the 4NQO-induced mutational signature to the 30 mutational signature available in COSMIC database version 2; the 4NQO-induced mutational signature presents a cosine similarity closer to signature 4 (tobacco smoking; 0.9) than to signature 29 (tobacco chewing; 0.81).

digestive tract carcinogenesis in mice. However, no information is available for the genome integrity of K14 beta-3 HPV49 E6/E7 Tg mice upon exposure to 4NQO treatment.

In this study, we perform whole-exome sequencing of upper-digestive tract lesions of different K14 HPV E6/E7 Tg animals and show that HPV49 E6 and E7 strongly increase the accumulation of 4NQO-induced DNA mutations.

2. Materials and methods

2.1. Animal models and ethics statement

All Tg animal models used in this study have been previously described (Viarisio et al., 2011, 2016, 2018) and https://mito.dkfz.de/mito/Animal%20line/10954, https://mito.dkfz.de/mito/Animal%20line/11244, and https://mito.dkfz.de/mito/Animal%20line/11245).

The animal facility of the German Cancer Research Center has been officially approved by the responsible authority (Regional Council of Karlsruhe, Schlossplatz 4–6, 76131 Karlsruhe, Germany) (file no. 35–9185.64). Housing conditions are thus in accordance with the German Animal Welfare Act (TierSchG) and EU Directive 425 2010/63/EU. Regular inspections of the facility are conducted by the Veterinary Authority of Heidelberg (Bergheimer Str. 69, 69115 Heidelberg, Germany). All experiments were in accordance with the institutional guidelines (designated veterinarian according to article 25 of Directive, 2010/63/EU and Animal Welfare Body according to article 27 of Directive, 2010/63/EU) and were officially approved by the Regional Council of Karlsruhe (file no. 35–9185.81/G-164/12).

2.2. 4NQO treatment

Experimental groups of 6-week-old female WT or K14 HPV E6/E7 Tg mice of type 16, 38, and 49 were treated as described previously (Viarisio et al., 2016) and https://mito.dkfz.de/mito/Tumor%20model/10635). Biopsies were taken from the upper digestive tract (tongue and esophagus) of both control and treated animals, used for DNA extraction (DNeasy Blood and Tissue Kit, Qiagen, Hilden, Germany) or fixed in 4% formaldehyde in phosphate-buffered saline for 24 h at room temperature, and embedded in paraffin. Sections of 5 µm were then stained with hematoxylin and eosin (H&E). The whole-exome sequencing was performed in the High-Throughput Sequencing unit of the Genomics & Proteomics Core Facility of the German Cancer Research Center (DKFZ) using Agilent SureSelect Whole Exome Kit.

The histological diagnosis was carried out in a blinded manner by a certified pathologist (CF).

2.3. Exome analysis

The quality of the raw reads was estimated with FastQC software

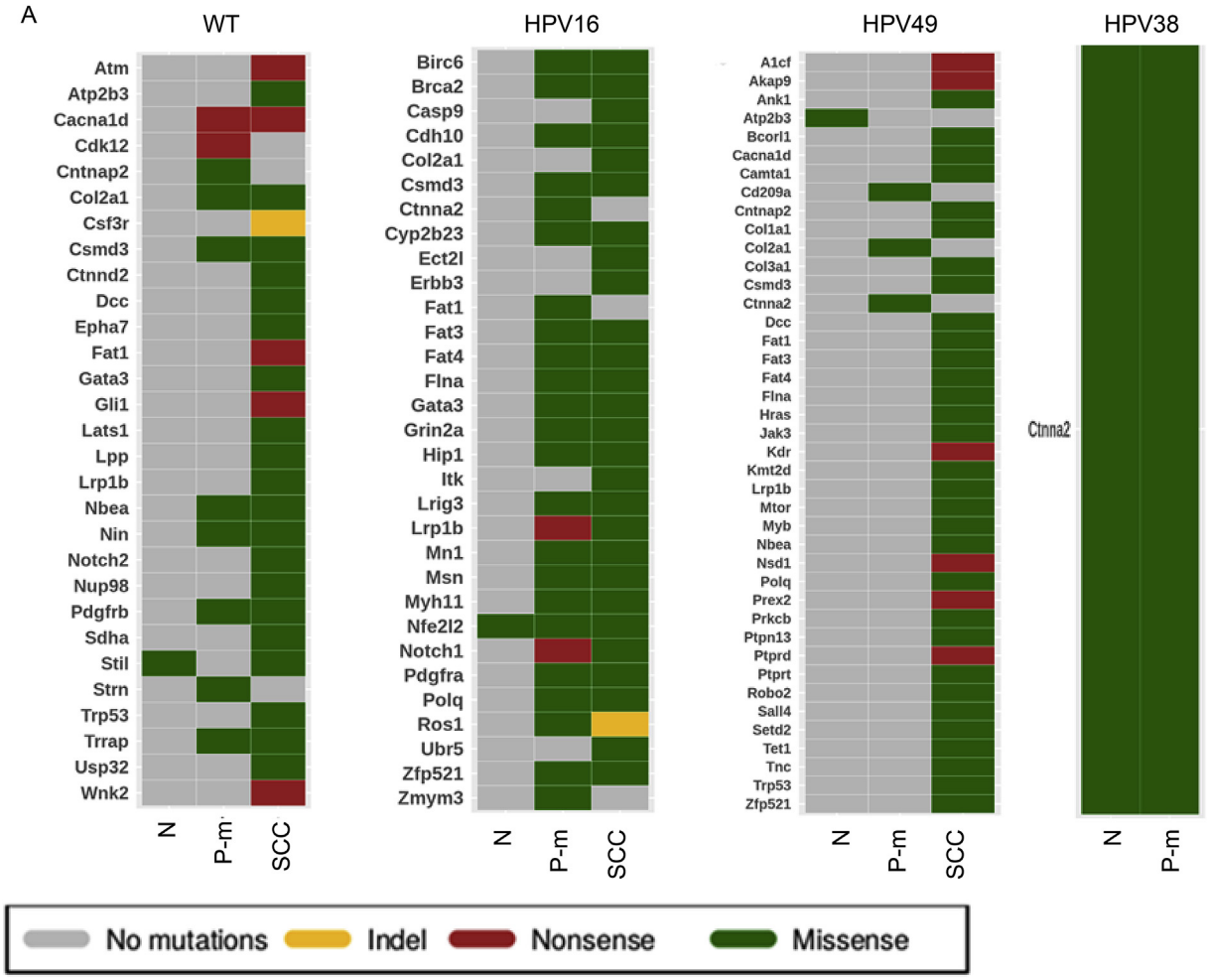

Fig. 4. Analyses of mutated genes in normal tissue and lesions from 4NQO-exposed Tg animals. (**A**) Heat-map of significantly mutated genes, corresponding to genes mutated in the corresponding sample and reported in the Cancer Gene Census list from the COSMIC database. The types of mutations indicated by colors are chosen according to the most prevalent mutation type in each sample. For categories with more than one sample (WT mice Normal: $n = 3$, HPV49 Tg mice Pre-m: $n = 2$, and HPV49 Tg mice SCC: $n = 4$), only the genes mutated in more than 50% of the samples are considered, and the type of mutation is defined as the most prevalent type among the samples. (**B**) Heatmap of significantly mutated genes, corresponding to genes mutated in the corresponding sample and reported to have an impact on epigenetic regulation processes. The types of mutations indicated by colors are chosen according to the most prevalent mutation type in each sample. For categories with more than one sample (WT mice Normal: $n = 3$, HPV49 Tg mice Pre-m: $n = 2$, and HPV49 Tg mice SCC: $n = 4$), only the genes mutated in more than 50% of the samples are considered, and the type of mutation is defined as the most prevalent type among the samples. (**C**) Heatmap of mutations in top genes mutated in human esophageal SCCs and their corresponding gene names in 4NQO-exposed animals. The types of mutation indicated by colors are chosen according to the most prevalent mutation type in each sample.

(version 0.11.5, http://www.bioinformatics.babraham.ac.uk/projects/fastqc/). Reads were mapped to the GRCm38 (mm10) mouse reference genome (ftp://hgdownload.cse.ucsc.edu/goldenPath/mm10/) using Burrows-Wheeler Aligner (version 0.7.15, http://bio-bwa.sourceforge.net/) and producing a BAM file. The following GATK Best Practice Recommendations were applied to the BAM files to improve variant detection quality. Picard (version 2.4.1, https://broadinstitute.github.io/picard/) SortSam was used to sort and index BAM files, and the AddOrReplaceReadGroups tool was used to replace all read groups with a single new read group. The duplicate reads were marked with the MarkDuplicates tool, and the newly produced BAM file was indexed with the BuildBamIndex tool. GATK (version 3.6.0, https://software.broadinstitute.org/gatk/download/) RealignerTargetCreator was used to determine the position concerned by local realignment, and IndelRealigner was used to perform local realignment around these sites. The GATK BaseRecalibrator tool was used to detect systematic errors in base quality scores. dbSNP and dbindel (version 142) for the GRCm38 (mm10) reference genome was downloaded from the Sanger website (ftp://ftp-mouse.sanger.ac.uk/REL-1505-SNPs_Indels/) and considered as input. Lastly, the index of the output BAM file was created with Picard BuildBamIndex, and GATK PrintReads was used to write out sequence read data.

The quality of the alignment was estimated with QualiMap (version 2.0.2, http://qualimap.bioinfo.cipf.es/). Then, the variant calling was done with MuTect2 (https://software.broadinstitute.org/gatk/documentation/tooldocs/3.6-0/org_broadinstitute_gatk_tools_walkers_cancer_m2_MuTect2.php) by using a skin sample from a WT mouse not exposed to 4NQO as the “normal sample” for paired analysis. Only somatic mutations passing the MuTect2 internal filters were considered for the analysis. The VCF files are annotated with Annovar by using the MutSpec-Annot tool in Galaxy (Ardin et al., 2016). Variants were then filtered based on SegDup databases from UCSC (version from 4 May 2014, http://hgdownload.cse.ucsc.edu/goldenPath/mm10/database/genomicSuperDups.txt.gz), as well as Tandem Repeat and RepeatMasker (version from 9 February 2012, http://hgdownload.soe.ucsc.edu/goldenPath/mm10/bigZips/) (Tables S1–17). House-made scripts were then used to keep only SNPs that have a functional impact and fall in exonic or splicing regions. NMF mutational signatures were

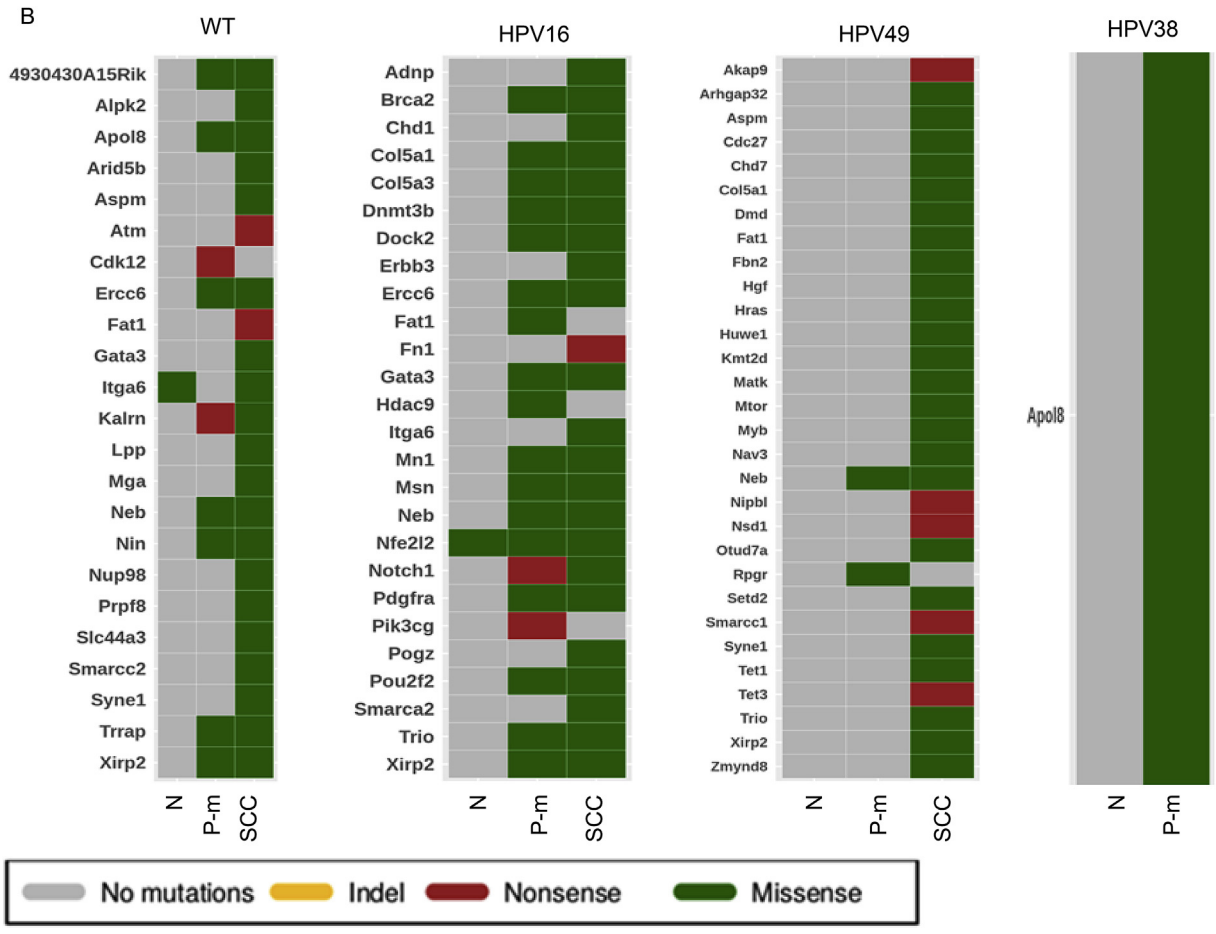

Fig. 4. (*continued*)

inferred with MutSpec-NMF tools, as previously reported.

The raw sequencing data has been deposited in Sequence Read Archive (NCBI) database, under the accession number PRJNA557836.

2.4. Comparison with epigenetic driver/modifier genes and Cancer Gene Census list

The list of epigenetic driver and modifier genes was constructed on the basis of genes reported in different publications (Gonzalez-Perez et al., 2013; Shen and Laird, 2013; Sturm et al., 2014; Timp and Feinberg, 2013; Vogelstein et al., 2013).

The Cancer Gene Census list was downloaded from the COSMIC website (March 2019, http://cancer.sanger.ac.uk/census).

The comparison of the mouse data with the human data was done with Bioconductor (release 3.6, https://www.bioconductor.org/) in R (version 3.4.4, codename "Someone to Lean On"). The top mutated genes in human esophagus SCC were retrieved from the Genomic Data Commons Data Portal (https://portal.gdc.cancer.gov/). The module BioMart (Durinck et al., 2005, 2009) (version 2.34.2) enables the conversion of 35 of the 40 (87.5%) top mutated human gene names to their corresponding mouse gene names using the Ensembl database (version 95). The heatmaps were generated considering the genes mutated in more than 50% of the analyzed samples, i.e. WT mice Normal: $n = 3$, HPV49 Tg mice Pre-m: $n = 2$, and HPV49 Tg mice SCC: $n = 4$).

2.5. Comparison with human cancer mutated genes

Data from human head and neck (HNC) cancers were retrieved from the Genomic Data Commons Data Portal (https://portal.gdc.cancer.gov/). Sample were selected for the following anatomical divisions: tonsil, oropharynx or base of the tongue. A gene was included in the analysis if mutated in at least one individual of the cohort considered. The module BioMart (Durinck et al., 2005, 2009) (version 2.34.2) enables the conversion of 6056 of the 7030 (86%) mutated mice gene names.

3. Results

3.1. Whole-exome sequencing analyses of upper digestive tract lesions from 4NQO-treated mice

To evaluate whether the high susceptibility of K14 beta-3 HPV49 E6/E7 Tg mice to 4NQO-induced cancers can be explained by their tendency to accumulate DNA mutations, we performed whole-exome sequencing (Illumina HiSeq). WT animals were included in the experiment as a comparative model. In addition, we selected a few specimens of 4NQO-treated K14 HPV16 or HPV38 E6/E7 Tg animals, which showed, respectively, high and low susceptibility to 4NQO-mediated carcinogenesis (Strati et al., 2006; Viarisio et al., 2016). As shown in Fig. 1, histologically confirmed specimens were selected from 4NQO-treated animals from two independent experiments (Viarisio et al., 2016) (Fig. 1). In the 4NQO-treated WT animals, only one SCC was detected and included in the whole-exome analysis, whereas 4NQO-treated K14 HPV38 E6/E7 Tg mice did not develop any SCC (Viarisio et al., 2016).

For the analysis of the DNA mutations in 4NQO-treated animals, the genomic sequence of the WT mouse not exposed to any type of treatment was determined in an independent experiment (Viarisio et al., 2018) and was used as a control sample in paired analysis. Exome

C

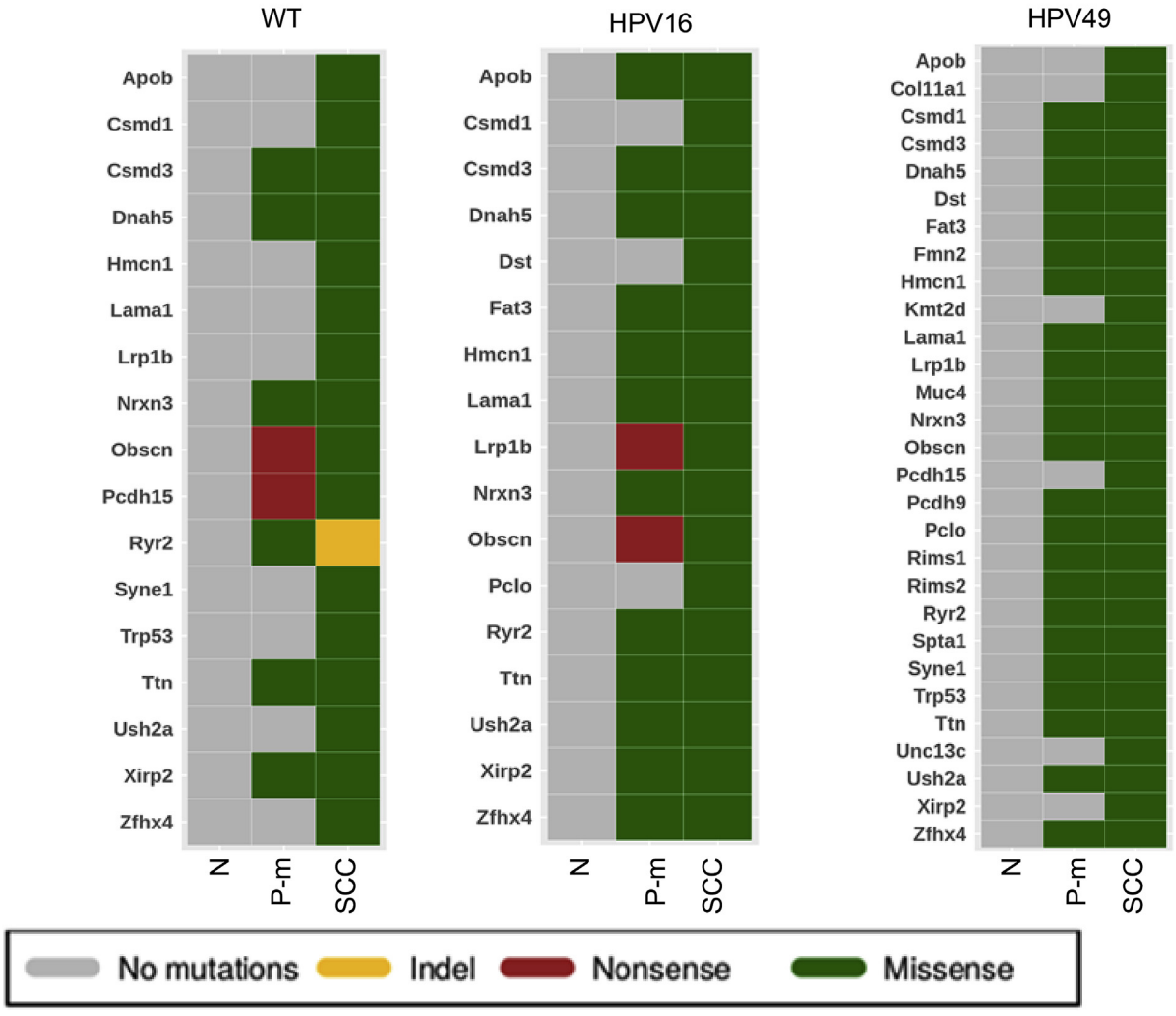

Fig. 4. (*continued*)

Table 1
Number and type of mutations in WT and Tg animals upon 4NQO treatments. Each specimen processed for whole exome sequencing was collected from different mice (n:17).

Mouse Number	Mouse Type	Tissue type	Histo-pathology	Mutect2[a] Somatic mutations (SNP; indels)	Number of mutated genes	Number of cancer gene census mutated (n = 801)	Number of cancer gene Epidriver/EpiModifier (n = 637)	Number of shared mutated genes in animals and human ESCA[b] (n = 40)
1	WT	Esophagus	Skin	**18** (18; 0)	**18**	**1**	**1**	**0**
2	WT	Esophagus	Skin	**13** (11; 2)	**13**	**1**	**0**	**0**
3	WT	Esophagus	Skin	**32** (30; 2)	**32**	**0**	**2**	**0**
4	WT	Esophagus	Pre-M	**739** (726; 13)	**694**	**37**	**27**	**10**
5	WT	Tongue	SCC	**2056** (2036; 20)	**1824**	**107**	**86**	**23**
6	HPV16	Esophagus	Skin	**14** (12; 2)	**14**	**1**	**1**	**0**
7	HPV16	Esophagus	Pre-M	**1657** (1640; 17)	**1505**	**73**	**58**	**17**
8	HPV16	Esophagus	SCC	**1943** (1931; 12)	**1723**	**93**	**78**	**23**
9	HPV38	Esophagus	Skin	**16** (14; 2)	**16**	**3**	**1**	**0**
10	HPV38	Esophagus	Pre-M	**324** (315; 9)	**316**	**14**	**14**	**5**
11	HPV49	Tongue	Skin	**12** (12; 0)	**12**	**2**	**0**	**0**
12	HPV49	Esophagus	Pre-M	**235** (234; 1)	**228**	**10**	**5**	**2**
13	HPV49	Esophagus	Pre-M	**2543** (2522; 21)	**2216**	**110**	**97**	**23**
14	HPV49	Esophagus	SCC	**3413** (3397; 16)	**2795**	**150**	**109**	**26**
15	HPV49	Esophagus	SCC	**3623** (3590; 33)	**2994**	**145**	**134**	**25**
16	HPV49	Esophagus	SCC	**2709** (2692; 17)	**2318**	**121**	**98**	**25**
17	HPV49	Esophagus	SCC	**1648** (1637; 11)	**1484**	**79**	**69**	**21**

[a] Mutect2 filtered mutations (see Methods for filtering parameters).
[b] ESCA: Esophageal Carcinoma.

sequencing of the collected samples generated an average coverage of 154.66 × ± 15.82 × (mean ± standard deviation). Normal tissue from all four types of animals contained a relatively low number of somatic mutations (18 ± 6.61) (mean ± standard deviation) (Fig. 2). In contrast, the number of somatic mutations increased according to the severity of the lesions (Fig. 2). In 4NQO-exposed Tg animals, the mutational load varied across our cohort of pre-malignant lesions, averaging 1102 somatic variants (range, 235–2547) or 4.67 ± 3.73 variants per Mb. The exome of the well-differentiated SCCs had a substantially higher number of variants, with an average of 2571 somatic variants (range, 1648–3638) or 11.89 ± 3.18 variants per Mb.

In conclusion, whole-exome sequencing revealed that K14 HPV16 and HPV49 E6/E7 Tg mice have a high susceptibility to the accumulation of DNA mutations induced by 4NQO treatment.

3.2. Characterization of DNA mutations in 4NQO-treated animals

Most of the somatic mutations detected in pre-malignant lesions and SCCs were C:G > A:T mutations (Fig. 3A) (Tables S1–17). The application of the non-negative matrix factorization (NMF) method enabled the extraction of the mutational signatures composed of 96 single base substitution types, considering the trinucleotide sequence context (one base upstream and one base downstream) (Fig. 3B). Next, we compared the mutational signature of 4NQO-treated K14 HPV49 E6/E7 Tg mice mice with the 30 mutational signatures available in COSMIC database version 2, by the cosine similarity method (Alexandrov et al., 2013; Olivier et al., 2014). The value of the cosine similarity obtained for the new signature is 0.9 for COSMIC signature 4 (tobacco smoking) and 0.8 for COSMIC signature 29 (tobacco chewing) (Fig. 3C).

To evaluate whether the somatic mutations detected in specimens from the 4NQO-treated animals have some biological relevance in the development of pre-malignant and malignant lesions, we compared the list of mutated genes in our animal models with one identified in the Cancer Gene Census (Futreal et al., 2004; Sondka et al., 2018). Cancer genes were found to be mutated in pre-malignant and malignant lesions from 4NQO-treated mice (Fig. 4A). In addition, the number of mutated cancer genes gradually increased in SCCs from WT, K14 HPV16 E6/E7 Tg, and K14 HPV49 E6/E7 Tg animals. Only one cancer gene was found mutated in the pre-malignant lesion of K14 HPV38 E6/E7 Tg animals.

Similar results were obtained when we analyzed the DNA mutations in epi-driver and epi-modifier genes (Gonzalez-Perez et al., 2013; Shen and Laird, 2013; Sturm et al., 2014; Timp and Feinberg, 2013; Vogelstein et al., 2013) (Fig. 4B). K14 HPV49 E6/E7 Tg animals showed higher number of mutated genes upon 4NQO exposure in comparison WT and the other HPV Tg mice (Table 1).

We have previously shown in K14 HPV38 E6/E7 Tg animals that the viral proteins acts an early stage of UV-induced skin carcinogenesis facilitating the accumulation of DNA mutations, but they are dispensable for the cancer cell growth after full development of cSCC (Viarisio et al., 2011; 2018). To evaluate whether HPV38 and HPV49 cooperates with UV and 4NQO, respectively, to alter a similar pattern of cellular genes/pathways in mouse carcinogenesis, we compared the DNA mutations of SCC from 4NQO-exposed HPV49 Tg mice and UV-exposed HPV38 Tg mice. We identified a large number of common mutations (n = 3705) in malignant lesions of both animal models, leading to alteration of similar cellular pathways (Fig. S1).

Finally, we compared the pattern of DNA mutations detected in lesions from 4NQO-exposed Tg animals with the pattern of mutations found in esophageal SCC in humans. As shown in Fig. 4C and Table 1, 29 of the 35 (83%) top genes mutated in human SCCs were found mutated in lesions from HPV49 E6/E7 Tg animals. In contrast, a lower number of these human genes were mutated in lesions from WT and K14 HPV16 E6/E7 Tg animals (Fig. 4C). In addition, we compared the pattern of mutations detected in SCC of 4NQO-exposed K14 HPV49 E6/E7 Tg animals with the pattern of mutations detected in human HNCSCC associated with tobacco, HPV infection or tobacco/HPV infection. The analysis revealed that a large proportion of genes mutated in human SCC were also detected in the SCC of the Tg animals (Fig. S2A). Accordingly, the pathway analysis showed that similar alterations occurred in human and mouse SCC (Fig. S2B).

In conclusion, HPV49 E6 and E7 expression in upper digestive tract epithelia favors the accumulation of 4NQO-induced DNA mutations that resemble the signature of tobacco exposure.

4. Discussion

In a previous study, we showed that beta-3 HPV49 E6 and E7 expression driven by K14 promoter in a Tg mouse model strongly cooperates with the carcinogen 4NQO in promoting cancer in the upper digestive tract (Viarisio et al., 2016). A similar scenario has been observed in a Tg mouse model for the mucosal HR HPV16 (Strati et al., 2006). The synergism between 4NQO and viral oncogene expression in promoting carcinogenesis appeared to be beta-HPV-type specific, because beta-2 HPV38 E6 and E7 weakly cooperated with 4NQO in the same Tg model, promoting only papillomas but never cSCC (Viarisio et al., 2016). The opposite situation was observed when K14 HPV38 and K14 HPV49 E6/E7 Tg mice were exposed to another protocol of carcinogenesis using UV radiation. Only HPV38 E6 and E7 expression in K14 HPV38 E6/E7 Tg mice was found to cooperate with UV irradiation in the development of cSCC (Viarisio et al., 2011, 2016, 2018). These different abilities of HPV38 and HPV49 E6 and E7 in the Tg mouse models may be explained by the different tissue tropism or intrinsic properties of the mouse tissue. However as regards to different tissue tropism, it is possible that these viruses, in order to efficiently complete their life cycle, may have developed specific mechanisms to counteract the anti-proliferative events induced by environmental factors at distinct anatomical sites. Interestingly, compelling lines of evidence from epidemiological and functional studies support the model that beta-1 and beta-2 HPV types play a role at an initial stage of skin carcinogenesis, facilitating the accumulation of UV-induced DNA mutations that, in turn, render cancer cell proliferation independent of the expression of viral genes. In line with this model, beta HPV DNA is not detected in all cancer cells, and the viral load decreases with the progression of the severity of the skin lesion (Correa et al., 2017; Dona et al., 2019; Weissenborn et al., 2005). Thus, specific beta HPV types may act with a hit-and-run mechanism in UV-induced cSCC development (Rollison et al., 2019). Based on the findings presented here, it is possible to speculate that a similar synergistic model could exist for other HPVs and environmental factors at different anatomical sites. Importantly, it could be possible that oral HPV infections may act with a hit-and-run mechanism in the development of a subset of HNC cancers.

A limitation of our study is the relatively small number of specimens that were subjected to whole-exome sequencing, especially for the K14 HPV16 and HPV38 E6/E7 Tg animals. However, the high susceptibility of K14 HPV49 E6/E7 animals to 4NQO-induced mutations was consistently observed in all mice in two independent experiments with 4NQO-exposed animals. Further epidemiological and biological studies are needed to evaluate the possible synergism of beta-3 HPV types and tobacco exposure in promoting any pathological condition in humans.

Conflicts of interest

The authors declare no competing financial interests.

Acknowledgments

We are grateful to all members of our laboratories at DKFZ and IARC for their cooperation, Nicole Suty for her help with preparation, and Dr Karen Müller for editing this manuscript.

The study was supported by a grant from Deutsche Krebshilfe, Germany (no. 110259) to LG and MT and Fondation ARC, France pour

la recherche sur le cancer (no. PJA 20151203192) (https://www.fondation-arc.org/espace-chercheur) and the Institut National de la Santé et de la Recherche Médicale, France (no. ENV201610) (https://www.eva2.inserm.fr/EVA/jsp/AppelsOffres/CANCER/) to MT.

We also thank the High-Throughput Sequencing unit of the Genomics & Proteomics Core Facility, German Cancer Research Center (DKFZ), for providing excellent sequencing services.

The authors alone are responsible for the views expressed in this article, and they do not necessarily represent the views, decisions, or policies of the institutions with which they are affiliated.

Appendix A. Supplementary data

Supplementary data to this article can be found online at https://doi.org/10.1016/j.virol.2019.09.010.

References

Alexandrov, L.B., Nik-Zainal, S., Wedge, D.C., Aparicio, S.A., Behjati, S., Biankin, A.V., Bignell, G.R., Bolli, N., Borg, A., Borresen-Dale, A.L., Boyault, S., Burkhardt, B., Butler, A.P., Caldas, C., Davies, H.R., Desmedt, C., Eils, R., Eyfjord, J.E., Foekens, J.A., Greaves, M., Hosoda, F., Hutter, B., Ilicic, T., Imbeaud, S., Imielinski, M., Jager, N., Jones, D.T., Jones, D., Knappskog, S., Kool, M., Lakhani, S.R., Lopez-Otin, C., Martin, S., Munshi, N.C., Nakamura, H., Northcott, P.A., Pajic, M., Papaemmanuil, E., Paradiso, A., Pearson, J.V., Puente, X.S., Raine, K., Ramakrishna, M., Richardson, A.L., Richter, J., Rosenstiel, P., Schlesner, M., Schumacher, T.N., Span, P.N., Teague, J.W., Totoki, Y., Tutt, A.N., Valdes-Mas, R., van Buuren, M.M., van 't Veer, L., Vincent-Salomon, A., Waddell, N., Yates, L.R., Australian Pancreatic Cancer Genome, I, Consortium, I.B.C., Consortium, I.M.-S., PedBrain, I., Zucman-Rossi, J., Futreal, P.A., McDermott, U., Lichter, P., Meyerson, M., Grimmond, S.M., Siebert, R., Campo, E., Shibata, T., Pfister, S.M., Campbell, P.J., Stratton, M.R., 2013. Signatures of mutational processes in human cancer. Nature 500, 415–421.

Ardin, M., Cahais, V., Castells, X., Bouaoun, L., Byrnes, G., Herceg, Z., Zavadil, J., Olivier, M., 2016. MutSpec: a Galaxy toolbox for streamlined analyses of somatic mutation spectra in human and mouse cancer genomes. BMC Bioinf. 17, 170.

Bottalico, D., Chen, Z., Dunne, A., Ostoloza, J., McKinney, S., Sun, C., Schlecht, N.F., Fatahzadeh, M., Herrero, R., Schiffman, M., Burk, R.D., 2011. The oral cavity contains abundant known and novel human papillomaviruses from the Betapapillomavirus and Gammapapillomavirus genera. J. Infect. Dis. 204, 787–792.

Cornet, I., Bouvard, V., Campo, M.S., Thomas, M., Banks, L., Gissmann, L., Lamartine, J., Sylla, B.S., Accardi, R., Tommasino, M., 2012. Comparative analysis of transforming properties of E6 and E7 from different beta human papillomavirus types. J. Virol. 86, 2366–2370.

Correa, R.M., Vladimirsky, S., Heideman, D.A., Coringrato, M., Abeldano, A., Olivares, L., Del Aguila, R., Alonio, L.V., Snijders, P.J., Picconi, M.A., 2017. Cutaneous human papillomavirus genotypes in different kinds of skin lesions in Argentina. J. Med. Virol. 89, 352–357.

Dona, M.G., Chiantore, M.V., Gheit, T., Fiorucci, G., Vescio, M.F., La Rosa, G., Accardi, L., Costanzo, G., Giuliani, M., Romeo, G., Rezza, G., Tommasino, M., Luzi, F., Di Bonito, P., 2019. Comprehensive analysis of beta and gamma Human Papillomaviruses in actinic keratosis and apparently healthy skin of elderly patients. Br. J. Dermatol. 18, 620–622.

Durinck, S., Moreau, Y., Kasprzyk, A., Davis, S., De Moor, B., Brazma, A., Huber, W., 2005. BioMart and Bioconductor: a powerful link between biological databases and microarray data analysis. Bioinformatics 21, 3439–3440.

Durinck, S., Spellman, P.T., Birney, E., Huber, W., 2009. Mapping identifiers for the integration of genomic datasets with the R/Bioconductor package biomaRt. Nat. Protoc. 4, 1184–1191.

Forslund, O., Johansson, H., Madsen, K.G., Kofoed, K., 2013. The nasal mucosa contains a large spectrum of human papillomavirus types from the Betapapillomavirus and Gammapapillomavirus genera. J. Infect. Dis. 208, 1335–1341.

Futreal, P.A., Coin, L., Marshall, M., Down, T., Hubbard, T., Wooster, R., Rahman, N., Stratton, M.R., 2004. A census of human cancer genes. Nat. Rev. Cancer 4, 177–183.

Gonzalez-Perez, A., Jene-Sanz, A., Lopez-Bigas, N., 2013. The mutational landscape of chromatin regulatory factors across 4,623 tumor samples. Genome Biol. 14, r106.

Hampras, S.S., Rollison, D.E., Giuliano, A.R., McKay-Chopin, S., Minoni, L., Sereday, K., Gheit, T., Tommasino, M., 2017. Prevalence and concordance of cutaneous beta human papillomavirus infection at mucosal and cutaneous sites. J. Infect. Dis. 216, 92–96.

Hasche, D., Vinzon, S.E., Rosl, F., 2018. Cutaneous papillomaviruses and non-melanoma skin cancer: causal agents or innocent bystanders? Front. Microbiol. 9, 874.

Ikenaga, M., Ishii, Y., Tada, M., Kakunaga, T., Takebe, H., 1975. Excision-repair of 4-nitroquinolin-1-oxide damage responsible for killing, mutation, and cancer. Basic Life Sci. 763–771 5b.

Olivier, M., Weninger, A., Ardin, M., Huskova, H., Castells, X., Vallee, M.P., McKay, J., Nedelko, T., Muehlbauer, K.R., Marusawa, H., Alexander, J., Hazelwood, L., Byrnes, G., Hollstein, M., Zavadil, J., 2014. Modelling mutational landscapes of human cancers in vitro. Sci. Rep. 4, 4482.

Pierce Campbell, C.M., Messina, J.L., Stoler, M.H., Jukic, D.M., Tommasino, M., Gheit, T., Rollison, D.E., Sichero, L., Sirak, B.A., Ingles, D.J., Abrahamsen, M., Lu, B., Villa, L.L., Lazcano-Ponce, E., Giuliano, A.R., 2013. Cutaneous human papillomavirus types detected on the surface of male external genital lesions: a case series within the HPV Infection in Men Study. J. Clin. Virol. 58, 652–659.

Rollison, D.E., Viarisio, D., Amorrortu, R.P., Gheit, T., Tommasino, M., 2019. An emerging issue in oncogenic virology: the role of beta human papillomavirus types in the development of cutaneous squamous cell carcinoma. J. Virol. 93.

Shen, H., Laird, P.W., 2013. Interplay between the cancer genome and epigenome. Cell 153, 38–55.

Sondka, Z., Bamford, S., Cole, C.G., Ward, S.A., Dunham, I., Forbes, S.A., 2018. The COSMIC Cancer Gene Census: describing genetic dysfunction across all human cancers. Nat. Rev. Cancer 18, 696–705.

Strati, K., Pitot, H.C., Lambert, P.F., 2006. Identification of biomarkers that distinguish human papillomavirus (HPV)-positive versus HPV-negative head and neck cancers in a mouse model. Proc. Natl. Acad. Sci. U. S. A. 103, 14152–14157.

Sturm, D., Bender, S., Jones, D.T., Lichter, P., Grill, J., Becher, O., Hawkins, C., Majewski, J., Jones, C., Costello, J.F., Iavarone, A., Aldape, K., Brennan, C.W., Jabado, N., Pfister, S.M., 2014. Paediatric and adult glioblastoma: multiform (epi)genomic culprits emerge. Nat. Rev. Cancer 14, 92–107.

Timp, W., Feinberg, A.P., 2013. Cancer as a dysregulated epigenome allowing cellular growth advantage at the expense of the host. Nat. Rev. Cancer 13, 497–510.

Tommasino, M., 2014. The human papillomavirus family and its role in carcinogenesis. Semin. Cancer Biol. 26, 13–21.

Tommasino, M., 2017. The biology of beta human papillomaviruses. Virus Res. 231, 128–138.

Torres, M., Gheit, T., McKay-Chopin, S., Rodriguez, C., Romero, J.D., Filotico, R., Dona, M.G., Ortiz, M., Tommasino, M., 2015. Prevalence of beta and gamma human papillomaviruses in the anal canal of men who have sex with men is influenced by HIV status. J. Clin. Virol. 67, 47–51.

Van Doorslaer, K., Bernard, H.U., Chen, Z., de Villiers, E.M., zur Hausen, H., Burk, R.D., 2011. Papillomaviruses: evolution, Linnaean taxonomy and current nomenclature. Trends Microbiol. 19, 49–50 author reply 50-41.

Van Doorslaer, K., Tan, Q., Xirasagar, S., Bandaru, S., Gopalan, V., Mohamoud, Y., Huyen, Y., McBride, A.A., 2013. The Papillomavirus Episteme: a central resource for papillomavirus sequence data and analysis. Nucleic Acids Res. 41, D571–D578.

Viarisio, D., Mueller-Decker, K., Kloz, U., Aengeneyndt, B., Kopp-Schneider, A., Grone, H.J., Gheit, T., Flechtenmacher, C., Gissmann, L., Tommasino, M., 2011. E6 and E7 from beta HPV38 cooperate with ultraviolet light in the development of actinic keratosis-like lesions and squamous cell carcinoma in mice. PLoS Pathog. 7, e1002125.

Viarisio, D., Muller-Decker, K., Accardi, R., Robitaille, A., Durst, M., Beer, K., Jansen, L., Flechtenmacher, C., Bozza, M., Harbottle, R., Voegele, C., Ardin, M., Zavadil, J., Caldeira, S., Gissmann, L., Tommasino, M., 2018. Beta HPV38 oncoproteins act with a hit-and-run mechanism in ultraviolet radiation-induced skin carcinogenesis in mice. PLoS Pathog. 14, e1006783.

Viarisio, D., Muller-Decker, K., Zanna, P., Kloz, U., Aengeneyndt, B., Accardi, R., Flechtenmacher, C., Gissmann, L., Tommasino, M., 2016. Novel ss-HPV49 transgenic mouse model of upper digestive tract cancer. Cancer Res. 76, 4216–4225.

Vogelstein, B., Papadopoulos, N., Velculescu, V.E., Zhou, S., Diaz Jr., L.A., Kinzler, K.W., 2013. Cancer genome landscapes. Science 339, 1546–1558.

Weissenborn, S.J., Nindl, I., Purdie, K., Harwood, C., Proby, C., Breuer, J., Majewski, S., Pfister, H., Wieland, U., 2005. Human papillomavirus-DNA loads in actinic keratoses exceed those in non-melanoma skin cancers. J. Investig. Dermatol. 125, 93–97.